Vratislava Mošová

Why are the meshless methods used?

In: Jan Chleboun and Karel Segeth and Tomáš Vejchodský (eds.): Programs and Algorithms of Numerical Mathematics, Proceedings of Seminar. Prague, May 28-31, 2006. Institute of Mathematics AS CR, Prague, 2006. pp. 202–207.

Persistent URL: http://dml.cz/dmlcz/702838

WHY ARE THE MESHLESS METHODS USED?

Vratislava Mošová

1. A bit about meshless methods

Meshless (or meshfree) methods are a useful tool for solving partial differential equations. These methods are often compared with the Finite Element Methods. The FEM are essentially applications of the Galerkin method to the weak formulation of a given problem and use spline spaces as approximating subspaces. The basic difference between the FEM and the meshless methods consists in the construction of the approximating space. In the meshless methods, this space is formed by shape functions. The following property plays a fundamental role in construction of these functions.

Definition 1 Let $x_1, x_2, \ldots, x_N$ be arbitrarily spaced points (called particles) in the domain $\Omega \subset R^n$. The functions $\{\Psi_I\}_{i=1}^N$ that are defined on Ω form the partition of unity of s consistency if for every monomial $p(x) \in \mathcal{P}_s$

$$\sum_{I=1}^{N} \Psi_I(x) p(x_I) = p(x) \quad \forall x \in \Omega. \tag{1}$$

Different meshless methods construct the partition of unity in different ways. Shape functions in Smooth Particle Hydrodynamic Method (SPHM, see [10]), Reproducing Kernel Particle Method (RKPM, see [4], [5]), and Reproducing Kernel Hierarchical Partition of Unity Method (RKHPUM, see [9]) are derived to reproduce the kernel (in the integral form) of the approximated functions. Diffuse Element Method (DEM, see [11]) and Element-Free Galerkin Method (EFGM, see [3]) are based on a moving least squares procedure. Partition of Unity (PU, see [1]), *hp*-clouds (see [7]) and Generalized Finite Element Method (GFEM, see [1], [2]) are methods where functions from the approximating space are products of functions from an extrinsic basis (its components form a partitition of unity) and from an intrinsic basis (its components include important features of the solution in the approximation space).

In this contribution, we give some illustrative examples and we study the behaviour of their solutions obtained by means of the FEM, the RKPM and the RKHPUM, and then we show some problems that can be successfully solved by means of meshless methods.

2. Meshless methods and solution of Helmholtz equation

Example 1 Consider the following 1D boundary value problem:

$$u''(x) + 16^2 u(x) = x, \quad x \in (0,1), \tag{2}$$

$$u'(0) = u'(1) = 0. \tag{3}$$

We seek a weak solution of the given problem, it means $u \in W^{1,2}(0,1)$ such that

$$-\int_0^1 (u'v')\,\mathrm{d}x + 16^2 \int_0^1 uv\,\mathrm{d}x = \int_0^1 xv\,\mathrm{d}x, \ \forall v \in W^{1,2}(0,1). \tag{4}$$

a) Figure 1 shows the situation when we solve problem (2), (3) by the FEM with N=11 nodes and linear approximation of solution. This solution is very poor. Let u be the exact solution and $\overline{u}$ its FEM approximation. The dependence of the approximation error $\max_x|u-\overline{u}|$ on the number of nodes is given in Figure 2. Note that the accuracy can be significantly improved if we use a cubic spline approximation of the solution.

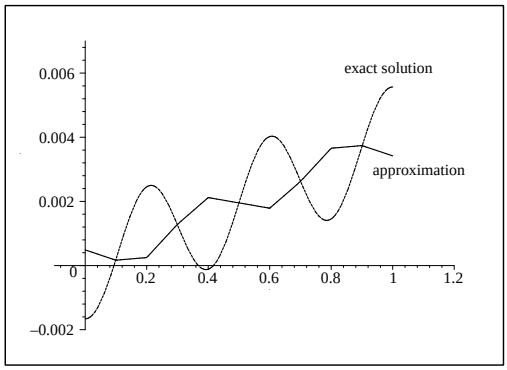

Fig. 1: *FEM – the approximation and the exact solution*

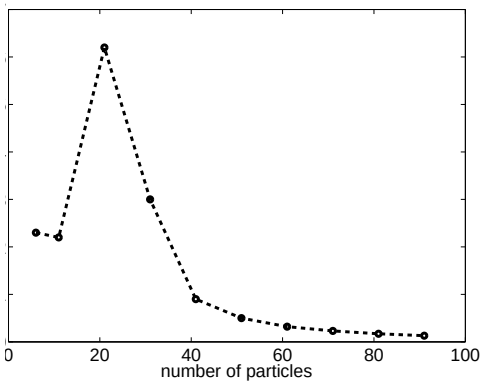

Fig. 2: *FEM – dependence of the approximation error on the number of nodes*

b) We find an approximation of the weak solution of equation (4) by means of the RKPM now. Suppose that uniformly distributed particles $x_1, \ldots x_N \in \langle 0,1\rangle$, the polynomial basis $p(x) = (1, x)$, the weight function

$$w(x) = \begin{cases} (1-x^2)^2 & \text{for } |x| < 1, \\ 0 & \text{otherwise,} \end{cases}$$

and a dilatation parametr R are given. Then the shape functions have the form

$$\Psi_I(x) = p\left(\frac{x-x_I}{R}\right)\, b(x_I)\, w\left(\frac{x-x_I}{R}\right), \ I = 1, \ldots N. \tag{5}$$

Here b is the solution of the system $M(x)b(x) = (1,0)^T$ with the moment matrix

$$M(x) = \begin{pmatrix} m_0(x) & m_1(x) \\ m_1(x) & m_2(x) \end{pmatrix}, \quad m_i(x) = \int_0^1 (y-x)^i w\left(\frac{y-x}{R}\right) \mathrm{d}y, \quad i = 0,1,2. \tag{6}$$

If we replace u in the weak formulation (4) by its approximation $\overline{u}(x) = \sum_{I=1}^{N} \Psi_I(x) U_I$ and v by $\Psi_J(x)$ for $J = 1, \ldots, N$, we receive the system of linear equations

$$A\,U = f,$$

where $U = (U_1, ..., U_N)^T$, $f = (f_1, \ldots, f_N)^T$, $f_I = \int_0^1 x\Psi_I(x)\,\mathrm{d}x$,

$$A = (a_{I,J})_{I,J=1}^{N}, \quad a_{I,J} = \int_0^1 \left(16^2 \Psi_I(x)\Psi_J(x) - \Psi_I'(x)\Psi_J'(x)\right) \mathrm{d}x.$$

The approximation $\overline{u}$ for $N = 11$, $R = 0.3$, and the exact analytical solution u are drawn in Figure 3. The behaviour of the error $|u - \overline{u}|$ is ilustrated in Figure 4.

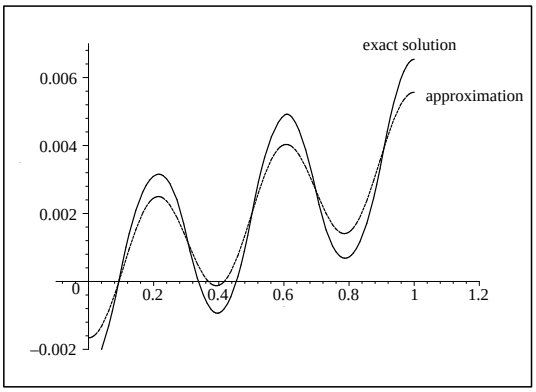

Fig. 3: *RKPM – the approximation and the exact solution*

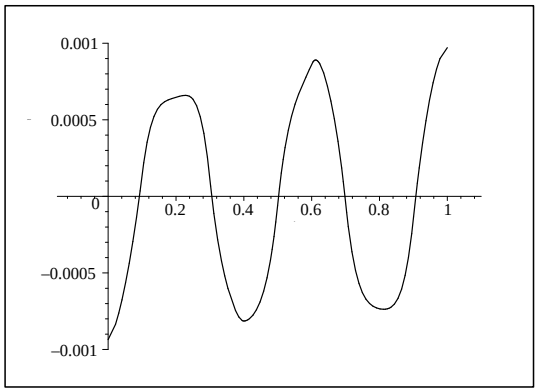

Fig. 4: *RKPM – the error $\overline{u} - u$*

c) We receive a better approximation if we solve the given problem by means of the RKHPUM. In this case, the following shape functions are constructed:

$$\Psi_I^0(x) = p\left(\frac{x-x_I}{R}\right) b^0(x_I)\, w\left(\frac{x-x_I}{R}\right), \; \Psi_I^1(x) = p\left(\frac{x-x_I}{R}\right) b^1(x_I)\, w\left(\frac{x-x_I}{R}\right),$$

where b^0, b^1 are solutions of the systems $M(x)b^0(x) = (1,0)^T$, $M(x)b^1(x) = (0,1)^T$ and the moment matrix M has the form (6). We insert the approximation

$$\overline{u}(x) = \sum_{I=1}^{11} \Psi_I^0(x) U_I^0 + \sum_{I=2}^{10} \Psi_I^1(x) U_I^1$$

into the weak formulation (4) and solve the resulting linear system. We can see in Figure 5 and Figure 6 that the accuracy of the solution has improved considerably.

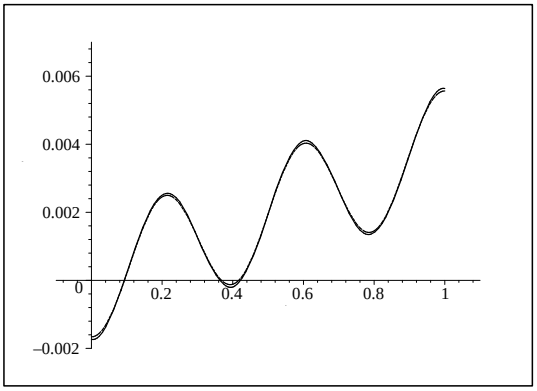

Fig. 5: *RKHPUM – the approximation and the exact solution*

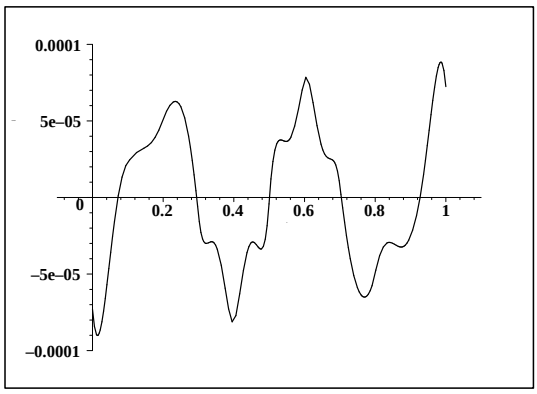

Fig. 6: *RKHPUM – the error* $\overline{u} - u$

Example 2 Let $\Omega = \langle 0,1\rangle \times \langle 0,1\rangle$,

$$\Delta u(x,y) + 16^2 u(x,y) = 1 \quad \text{in } \Omega, \tag{7}$$

$$\frac{\partial u(x,y)}{\partial n} = 2 \quad \text{on } \partial\Omega. \tag{8}$$

We seek a weak solution of this problem, it means $u \in W^{1,2}(\Omega)$ such that

$$-\iint_\Omega \nabla u \nabla v \,\mathrm{d}x\,\mathrm{d}y + \int_{\partial\Omega} 2v \,\mathrm{d}s + 16^2 \iint_\Omega uv \,\mathrm{d}x\,\mathrm{d}y = \iint_\Omega 1v \,\mathrm{d}x\,\mathrm{d}y, \ \forall v \in W^{1,2}(\Omega). \tag{9}$$

We develop the approximation of this solution by means of the RKHPUM for particles (x_I, y_I), $I = 1,\ldots,N$, uniformly distributed inside Ω, the polynomial basis $p(x,y) = (1,x,y)$, a dilatation parametr R, and the weight function

$$w(x,y) = \begin{cases} ((1-x^2)(1-y^2))^2 & \text{for } |x| \le 1,\ |y| \le 1, \\ 0 & \text{otherwise.} \end{cases}$$

In this case, the shape functions are of the form

$$\Psi_I^\alpha(x,y) = p\Big(\frac{x-x_I}{R}, \frac{y-y_I}{R}\Big) b^\alpha(x_I,y_I)\, w\Big(\frac{x-x_I}{R}, \frac{x-y_I}{R}\Big),$$

for $\alpha = (0,0),(1,0),(0,1)$, where vectors b^α satisfy $M(x,y)b^{(0,0)}(x,y) = (1,0,0)^T$, $M(x,y)b^{(1,0)}(x,y) = (0,1,0)^T$, $M(x,y)b^{(0,1)}(x,y) = (0,0,1)^T$, with

$$M(x,y) = \begin{pmatrix} m_{00}(x,y) & m_{10}(x,y) & m_{01}(x,y) \\ m_{10}(x,y) & m_{20}(x,y) & m_{11}(x,y) \\ m_{01}(x,y) & m_{11}(x,y) & m_{02}(x,y) \end{pmatrix}, \tag{10}$$

$$m_{ij}(x,y) = \iint_\Omega \left(\frac{\tilde{x}-x}{R}\right)^i \left(\frac{\tilde{y}-y}{R}\right)^j w\left(\frac{\tilde{x}-x}{R}, \frac{\tilde{y}-y}{R}\right) \mathrm{d}\tilde{x}\,\mathrm{d}\tilde{y}, \ i,j = 0,1,2. \tag{11}$$

Here we put

$$\overline{u}(x,y) = \sum_{I=1}^{N} \Psi_I^{(0,0)}(x,y) U_I^{(0,0)} + \sum_{I=1}^{N} (\Psi_I^{(1,0)}(x,y) U_I^{(1,0)} + \Psi_I^{(0,1)}(x,y) U_I^{(0,1)}) \qquad (12)$$

into the weak formulation (9) and solve the resulting system of linear equations. The graph of the approximation for $N = 100$ is plotted in Figure 7. This graph is very close to the graph of the analytical solution. The approximation errors $\sqrt{\sum_{i=0}^{20}\sum_{j=0}^{20}(u(\frac{i}{20},\frac{j}{20}) - \overline{u}(\frac{i}{20},\frac{j}{20}))^2} / \sqrt{\sum_{i=0}^{20}\sum_{j=0}^{20}(u(\frac{i}{20},\frac{j}{20}))^2}$ are depicted in Figure 8. The RKHPUM approximation $\overline{u}$ is computed for 25,36,49,64,100 particles.

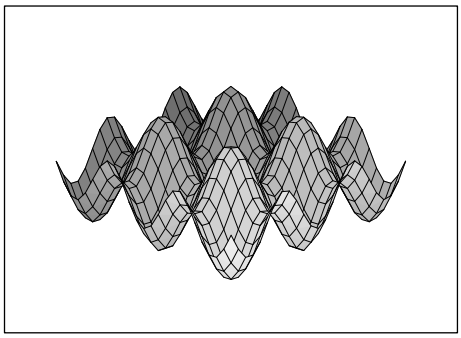

Fig. 7: *RKHPUM approximation ($N = 100$)*

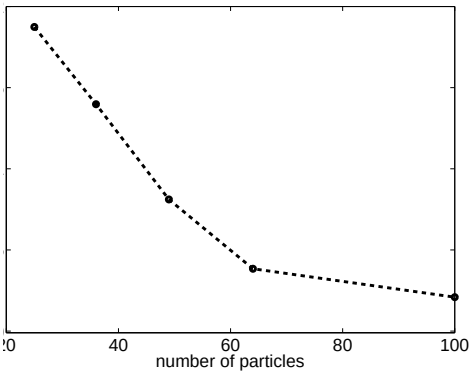

Fig. 8: *RKHPUM – dependence of the approximation error on the number of nodes*

3. Properties and advantages of the meshless methods

We demonstrated the construction of shape functions by means of the RKPM and the RKHPUM in the examples above. We saw that the considered meshless methods produce quite accurate results for $h = 0.1$. To achieve similar or even higher accuracy, we needed a number of particles that was significantly lower than the number of FEM nodes.

To realize meshless methods, no explicitly given mesh is required. The construction of shape functions needs no connectivity information. The size of support and smoothness of shape functions depend on the given dilatation parameter and on the chosen weight function only. The fact that no mesh has to be generated is appreciated in solving 3D structural mechanics problems (see [7]), in dealing with large deformations (see [4], [5]), or when we work with data received from computer tomography (CT) or magnetic resonance imaging (MRI) (see [6]).

The second advantage of meshless methods consists in the range in which shape functions can be constructed. It is possible to build shape functions with high regularity and to successfully solve higher order differential equations (see [8]) or to define shape functions that respect the local behaviour of the solution (see [12], [2]).

The meshless methods can be understood as an alternative to the FEM. For "simple" problems it is better to use the FEM, but in the specific problems mentioned above we prefer the meshless methods.

References

[1] I. Babuška, U. Banerjee, J.E. Osborn: *Survey of meshless and generalized finite element methods: An unified approach.* Acta Numer., 2003, 1–125.

[2] I. Babuška, J.M. Melenk: *The partition of unity finite element method: Basic theory and application.* Comput. Methods Appl. Mech. Engrg. **139**, 1996, 289–314.

[3] T. Belytschko, Y. Lu, I. Gu: *Element-free Galerkin methods.* Internat. J. Numer. Methods Engrg. **37**, 1994, 229–256.

[4] J.S. Chen, C. Pan, C.T. Wu, W.K. Liu: *Reproducing kernel particle methods for large deformation analysis of non-linear structures.* Comput. Methods Appl. Mech. Engrg. **139**, 1996, 195–227.

[5] J.S. Chen, C. Pan, C.T. Wu: *Large deformation analysis of rubber based on a reproducing kernel particle methods.* Comput. Mech. **19**, 1997, 211–227.

[6] E. Cueto, M. Doblaré, L. Gracia: *Imposing essential boundary conditions in the natural element method by means of density-scaled α-shapes.* Internat. J. Numer. Methods Engrg. **49**, 2000, 519–546.

[7] C.A. Duarte, I. Babuška, J.T. Oden: *Generalized finite element methods for three-dimensional structural mechanics problems*, 1999, `http://www.comco.com`.

[8] P. Joyot, J. Trunzier, F. Chinesta: *Enriched reproducing kernel approximation: Reproducing functions with discontinuous derivatives.* Meshfree methods for partial differential equations II, Springer, Berlin, 2004, 93–107.

[9] S. Li, W.K. Liu: *Reproducing kernel hierarchical partition of unity.* Internat. J. Numer. Methods Engrg. **45**, 1999, 251–317.

[10] J.J. Monaghan: *Why particle methods work.* Sci. Stat. Comput. **3**, 1982, 422–433.

[11] B. Nayroles, G. Touzot, P. Vilon: *Generalizing the finite element method: Diffuse approximation and diffuse elements.* Comput. Mech. **10**, 1992, 307–318.

[12] T. Strouboulis, I. Babuška, K. Copps: *The design and analysis of the generalized finite element method.* Comput. Methods Appl. Mech. Engrg. **181**, 2000, 43–69.